SIC based Secondary Coexistence over ATSC 3.0 Broadcast Channels

Rajrshi Dubey and Swades De
Department of Electrical Engineering and Bharti School of Telecommunication
Indian Institute of Technology Delhi, New Delhi 110016, India

***Abstract*—Coexistent communication, wherein multiple networks with dissimilar transmit waveform properties are deployed over the same band, has attracted a lot of recent attention, because of its high spectral efficiency. One of the most promising primary system candidates for such a deployment is over the ATSC 3.0 signaling based digital television broadcast transmission bands due to the excellent propagation characteristics. The throughput of the secondary system in such a deployment scenario suffers because of the high interference power from the broadcaster. Moreover, the secondary transmission parameters are chosen in such a way that the Quality of Service (QoS) of the primary network does not degrade. This paper investigates the feasibility of secondary network communication, under such a hostile scenario, using Successive Interference Cancellation (SIC) techniques. Various factors that contribute to the error in SIC systems are studied both analytically as well as through simulations. Based on the analysis, two schemes, namely, secondary slot size reduction and symbol blanking, are proposed for improving SIC performance. The performance of these schemes are analyzed in terms of the error vector magnitude of the primary network's estimated channel and its bit error rate. Through simulations it is also shown that, by using the proposed schemes, the secondary network is able to communicate at as low as -40 dB carrier-to-interference ratio.**

***Index Terms*—ATSC 3.0, coexistent communication, new radio (NR), successive interference cancellation (SIC)**

I. Introduction

The current spectrum will not be able to support the demands of the growing population of data-hungry devices. Moreover, this will put additional strain on the scarce bandwidth resource. There are essentially two sorts of solutions available to meet the constantly growing demands. The first solution attempts to utilize the unallocated spectrum at a higher frequency, e.g. millimeter wave band (mmWave). However, the mmWave network suffers from high path loss which is mitigated through the use of beamforming and dense deployment of cells. The small size of antennas at high frequency enables close packing of multiple antennas which facilitates narrow beamforming. The disadvantage of this approach is that it necessitates the dense deployment of cells, which is impractical in sparsely inhabited regions like rural areas. The second solution attempts to enhance the spectral efficiency of the pre-allocated lower frequency bands through parallel deployment of multiple communication technologies on the same time and frequency resources. This paper focuses on the second approach, and particularly studies coexistent communication in the digital terrestrial television (DTT) bands.

II. Background and Motivation

From the perspective of coexistent communication, the lower part of ultra high frequency band (UHF) is of particular interest due to its outstanding propagation characteristics owing to low propagation path loss. Since the license for this part of spectrum belongs to the television broadcasting services, they are considered as the primary users (PU) while the elements of the other coexisting network are treated as secondary users (SU) of the band. The coexistent communication over licensed band can be classified into three categories namely, overlay, interweave, and underlay. In an overlay system, the PU shares its data with SU, which it utilizes to reduce the interference to the PU receiver. Whereas, in an interweave system the channel is used by SU, only when the PU network is silent, while in an underlay system, the channel is simultaneously used by both PU and SU networks, with SU power adjusted so that, it does not degrade the QoS of the PU network, i.e., the interference at the primary receiver due to the secondary user should not exceed a threshold limit. In contrast, the SU has to tolerate the QoS degradation due to interference from the PU network.

Multiple studies have investigated the possibility of secondary communications by cognitive radio networks (CRN) on TV bands. The studies presented in [1]–[4] examine and employ TV white spaces (TVWS) for secondary network communication. The authors of [5]–[8] investigated data transmission by CRN on a licensed band through dynamic spectrum access. These studies utilizes TVWS for communication which usually lies in the paradigm of interweave type cognitive radio communication. However, these approaches are not suitable for urban areas due the the shortage of TVWS [3]. Overlay cognitive radio communication in DVB-T is studied in [20] but it requires cooperation between the PU and SU networks, whereas, the underlay communication does not require such overhead but the SU network needs to adjusts its parameters such that the QoS of PU does not degrade. The study in [9] determined $\frac{C}{I}$ protection ratios for varying degrees of signal overlap in DTT and LTE-A coexistent system. The authors in [10] evaluated protection ratios for coexisting digital video broadcast - terrestrial second generation (DVB-T2) and IEEE 802.22 WRAN networks. The optimum LTE operating configurations for different degrees of spectral overlap were evaluated in [11] with DVB-T2 lite system.

Ensuring good QoS is difficult for SU network as a con-

sequence of the maximum admissible interference constraint at PU receiver. Numerous researchers have looked into the possibility of enhancing QoS of Orthogonal Frequency Division Multiplexing (OFDM) based SU networks operating in TV broadcast environments. The authors in [12] devised a scheme that tunes SU transmit waveform parameters to attain its service target, while maintaining interference within limit at PU receiver. The study in [13] demonstrated that SU's performance can be enhanced if it is aware of the locations of PU receivers. The drawback of these studies is that they only focus on SU's transmitter parameters while completely ignoring any possibility of improvement at SU receiver.

One of the ways to improve SU performance is by applying interference cancellation. Improvement in spectrum efficiency of a system through the use of Interference cancellation (IC) is shown in [14]. Multiple studies have anlyzed IC techniques for nullifying cross technology interference. Technology independent multiple-output (TIMO) [15] and ZIMO [16] utilizes multiple antennas and assumes clean reference signal to eliminate cross technology interference. One of the bottleneck in applying IC technique is the unavailability of clean reference signal. The study in [17] leverages multiple antennas, RF frontends, and analog-to-digital converters (ADC) in a user equipment (UE) for handling the issue of unclean reference signals in a co-existing WiFi and LTE networks. However, these methods are only limited to multiple input single output (MISO) or multiple input multiple output (MIMO) systems and cannot cater to single input singe output (SISO) systems. The authors in [18] proposed an SIC scheme for Inter-Numerology Interference (INI) cancellation in windowed OFDM system while authors in [19] developed an SIC scheme for multi-numerology non-orthogonal multiple access (NOMA) system. However, both of these fail to account for realistic constraints such as pilot signal contamination and technical constraints set by specifications like fixed positions and limited number of pilot signals. Moreover, these solutions assume common sampling rate for the coexisting waveforms which is not feasible in our case, as the sub-carrier spacings are not integer multiple of each other. The study in [20] proposed an overlay scheme to enhance SIC performance in coexisting DVB-T and LTE network, the downside of the scheme is that it increases overhead at SU transmitter.

Since most of the schemes to improve the SIC performance in literature are either based on multiple antennas at the receiver or uses an overlay scheme which increases the overhead at the SU transmitter. Consequently, these schemes cannot be directly applied to SISO underlay scenario. Therefore, this paper proposes two schemes for improving the performance of the SIC module in NR-like SU receiver which is co-deployed in ATSC 3.0 band. The schemes aid in reducing pilot contamination and hence boost the SU network performance in an underlay system without using additional antennas. It can be observed from the simulation results that the combination of the two schemes yield BER close to zero between $\frac{C}{I}$ ratio of -40 to -20 dB.

The rest of the paper is organized as follows. Section II describes the system model alongwith SU receiver structure and its operation. Section III describes the proposed schemes. The simulation findings are discussed in Section IV. The paper is concluded in Section V.

III. System Model

The system model consists of an ATSC 3.0 based PU coexisting with an NR-like SU as shown in figure 1. Both PU and SU network share the same center frequency and spectrum. It is assumed that the parameters of the PU's transmitted waveform like FFT size, cyclic prefix (CP) length, sampling rate, subcarrier spacing, pilot symbols and their locations are known to the SU receiver. It is also assumed that the SU transmitter is time synchronized with the PU transmitter and the SU receiver is operating at high Signal-to-Noise Ratio (SNR) but low Signal-to-Interference ($\frac{S}{I}$) region. The continuous time transmit waveform for PU and SU is

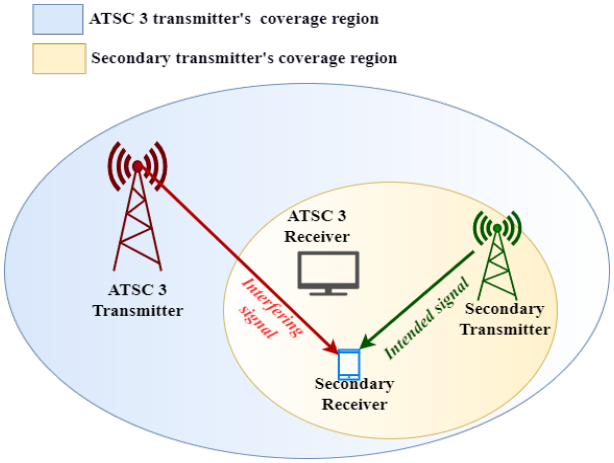

Fig. 1. ATSC 3.0 and secondary network coexistence scenario.

given by $x^a(t)$ and $x^l(t)$, respectively, where:

$$x^a(t) = \frac{\sqrt{P_a}\sum_{k=0}^{N^a-1} X_k^a e^{\frac{-j2\pi kt}{T_a^u}}}{\sqrt{T_a^u}} \Pi\left(\frac{t+T_a^g}{T_a}\right). \quad (1)$$

$$x^l(t) = \frac{\sqrt{P_l}\sum_{k=0}^{N^l-1} X_k^l e^{\frac{-j2\pi kt}{T_l^u}}}{\sqrt{T_l^u}} \Pi\left(\frac{t+T_l^g}{T_l}\right) \quad (2)$$

Here $x(t)$ denotes the time domain OFDM waveforms, T denotes the time duration of one OFDM symbol including CP, T^u denotes useful symbol duration, T^g denotes guard interval or CP duration, N denotes the number of active subcarriers including pilot subcarriers, X_k represents frequency domain data for k^{th} subcarrier, $\Pi(t)$ denotes the rectangle function of unit length, P denotes the transmitted power, N represents the FFT size, and the subscript or superscript a and l stands for ATSC 3 and secondary system, respectively. The system model assumes that during one symbol duration of PU only one slot of NR-like SU is allowed. Additionally, the data received at the SU receiver should not overlap with the CP of the PU (as shown in figure 2), which can be ensured

through synchronization between the PU and SU transmitters. Moreover, It is also assumed that the OFDM symbol length and FFT size of the SU waveform is much smaller than that of PU's, i.e., $T_l << T_a$ and $N_l << N_a$.

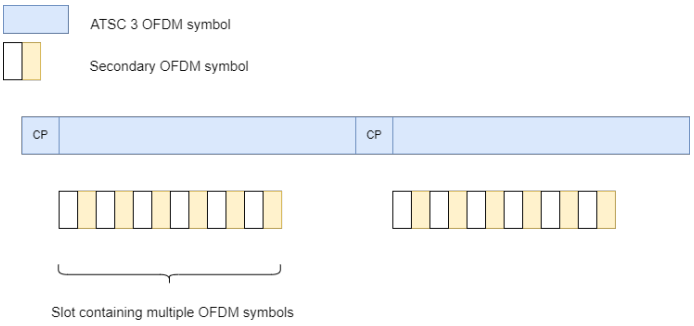

Fig. 2. Synchronized transmission by secondary network.

A. SU receiver structure

The receiver comprises two parts: - an interference regenerator chain that decodes and regenerates the ATSC 3.0 waveform and a SU decoder chain which is responsible for interference cancellation and decoding of SU data. Both the chains are equipped with ADCs working at their respective sampling rates. RF front end receives the waveform which

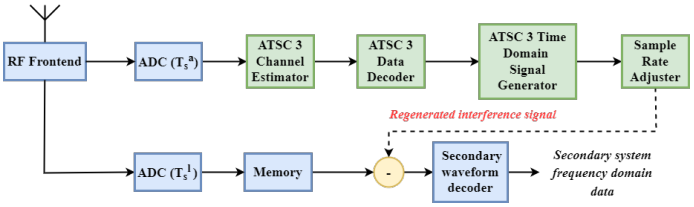

Fig. 3. SU receiver structure.

is sent parallely over both the chains, the received waveform in secondary decoder chain is first sampled by ADC and then stored in the memory unit whereas, in interference regenerator chain the received waveform is first digitized using ADC and subsequently its CP is discarded. The resultant signal is given by,

$$r(nT_a^s) = \frac{\sqrt{P_a}\sum_{k=0}^{N^a-1} H_k^a X_k^a e^{\frac{-j2\pi knT_a^s}{T_a^u}}}{\sqrt{T_a^u}}\Pi\left(\frac{nT_a^s}{T_a^u}\right) + \frac{\sum_{m\in\mathbb{Z}}\sqrt{P_l}\sum_{k=0}^{N^l-1} H_k^l[m]X_k^l[m]e^{\frac{-j2\pi knT_a^s}{T_l^u}}}{\sqrt{T_l^u}} \times \Pi\left(\frac{nT_a^s - mT_l + T_l^g}{T_l}\right) + n(t) \quad (3)$$

where H_k represents channel coeffecient on k^{th} subcarrier and m represents the number of SU OFDM symbols affected by a single ATSC 3.0 symbol, its maximum value is given by $\lfloor \frac{T_a^u}{T_l} \rfloor$.

B. Interference estimation

Since the receiver is operating in a high SNR region, therefore, the effect of AWGN noise on the system can be ignored. The interference estimation chain, process the waveform by treating the SU waveform as additive noise. On performing FFT the data received on k^{th} subcarrier is given by,

$$R(k) = \sqrt{P_a}\sum_{k=0}^{N^a-1} H_k^a X_k^a + \sum_{n=0}^{\frac{T_a^u}{T_a^s}}\left[\left(\frac{\sum_{m\in\mathbb{Z}}\sqrt{P_l}\sum_{k=0}^{N^l-1} H_k^l[m]X_k^l[m]e^{\frac{-j2\pi knT_a^s}{T_l^u}}}{\sqrt{T_l^u}} \times \Pi\left(\frac{nT_a^s - mT_l + T_l^g}{T_l}\right)\right)\right] e^{\frac{-j2\pi kn}{N_a}} \quad (4)$$

To eliminate the effect of the channel, frequency domain equalization is performed which requires estimates of the channel coefficients for each sub-carrier. This is facilitated through the use of pilot symbols. Let $X_\zeta = \{X_1, X_2, ..., X_P\}$ represent the set of P pilot symbols in a PU's OFDM symbol at sub-carrier locations $L = \{k^1, k^2, ..., k^P\}$. The channel for PU is computed using Least squares at these pilot locations which is given by, $\hat{H}(f) = \frac{R(f)}{X_f}$ where $f \in L$ and $X_f \in X_{zeta}$. The least-squares values obtained are then interpolated over the whole bandwidth to find the approximated channel coefficients at all the sub-carrier indices denoted by $\hat{H}$.

The estimated channel is then used for frequency-domain equalization whose output is fed to the constellation demapper to obtain the binary data. For interference regeneration, the binary data is again converted to a digitally modulated symbol using a constellation mapper. Let the reconstructed digital symbol be represented as $\hat{X}$. The $\hat{X}$ and $\hat{H}$ are fed to the ATSC 3.0 time-domain signal generator for interference regeneration denoted by $I(nT_a^s)$,

$$I(nT_a^s) = \frac{\sqrt{P_a}\sum_{k=0}^{N^a-1} \hat{H}_k^{\ a}\hat{X}_k^{\ a} e^{\frac{-j2\pi kn}{N_a}}}{\sqrt{T_a^u}}\Pi\left(\frac{nT_a^s}{T_a^u}\right) \quad (5)$$

For further processing, the sampling rate of regenerated interference is adjusted to match the sampling rate of the secondary system.

C. SU decoder chain

The processing of SU decoder chain begins with interference cancellation module. It takes in the rate adjusted regenerated interference and subtracts it from the data stored in memory. i.e., $s(nT_l^s) = r(nT_l^s) - I(nT_l^s)$,

$$s(nT_l^s) = \left(\frac{\sqrt{P_a}\sum_{k=0}^{N^a-1}({H_k}^a {X_k}^a - \hat{H_k}^a \hat{X_k}^a) e^{\frac{-j2\pi knT_l^s}{T_a^u}}}{\sqrt{T_a^u}} \times \Pi\left(\frac{nT_l^s}{T_a^u}\right)\right) + \left(\frac{\sum_{m\in\mathbb{Z}}\sqrt{P_l}\sum_{k=0}^{N^l-1} H_k^l[m]X_k^l[m] e^{\frac{-j2\pi knT_l^s}{T_l^u}}}{\sqrt{T_l^u}} \times \Pi\left(\frac{nT_l^s - mT_l + T_l^g}{T_l}\right)\right) \quad (6)$$

$$s(nT_l^s) = \left(\frac{\sum_{m\in\mathbb{Z}}\sqrt{P_l}\sum_{k=0}^{N^l-1} H_k^l[m]X_k^l[m] e^{\frac{-j2\pi knT_l^s}{T_l^u}}}{\sqrt{T_l^u}} \times \Pi\left(\frac{nT_l^s - mT_l + T_l^g}{T_l}\right)\right) + \Delta I(\hat{H}, \hat{X}) \quad (7)$$

Where $\Delta I(\hat{H}, \hat{X})$ represents residual interference. The secondary receiver chain uses equation (7) for further processing namely, pilot estimation, equalization and constellation demapping, etc.

D. Factors affecting SIC performance

The poor performance of SIC is caused by large values of residual interference. One of the causes of large value of residual interference is pilot contamination, which arises due to the use of the least-squares method for estimating channels at pilot subcarriers. The least-squares method is suitable for additive noise with low power, consequently, the estimates obtained do not track the actual channel coefficients. High residual interference is also caused by erroneous $\hat{X}$ which also arises as a result of pilot contamination in high SNR region. Their combined effect results into a non-zero value of $({H_k}^a {X_k}^a - \hat{H_k}^a \hat{X_k}^a)$ which is further amplified by the term $\sqrt{P_a}$ in $\Delta I(\hat{H}, \hat{X})$.

IV. Proposed Schemes

In this section, two schemes are proposed that helps in reducing pilot contamination and improves the performance of the SU receiver.

A. Reducing slot size of secondary system

Using the least-squares formula for channel estimation at pilot sub-carriers as described in section II.B and equation (4),

$$\hat{H}(f) = \frac{R(f)}{X_f} = \sqrt{P_a}H_f^a + \sum_{n=0}^{\frac{T_a^u}{T_a^s}} \left(\left(\frac{\sum_{m\in\mathbb{Z}}\sqrt{P_l}\sum_{k=0}^{N^l-1} H_k^l[m]X_k^l[m] e^{\frac{-j2\pi knT_a^s}{T_l^u}}}{X_f\sqrt{T_l^u}} \times \Pi\left(\frac{nT_a^s - mT_l + T_l^g}{T_l}\right)\right) e^{\frac{-j2\pi kn}{Na}} \right) \quad (8)$$

It can be seen from equation (8) that the contamination of the pilot at l^{th} sub-carrier is a function of the variable m, i.e., the number of SU OFDM symbols which occurs in one symbol duration of PU. Since we have assumed that within one symbol of PU, we can transmit only one slot of SU. Therefore, the pilot contamination can be lowered by decreasing the number of OFDM symbols in a slot.

B. By blanking secondary transmission during interference estimation

In this scheme, the SU transmitter remains silent for a PU's symbol duration during which the secondary receiver estimates the interference caused by the PU transmitter. The least-square estimation performs optimally in this case as residual interference terms vanishes at pilot sub-carriers, $\hat{H}(f) = \frac{R(f)}{X_f} = \sqrt{P_a}H_f^a$. In the subsequent symbols, the interference generation chain uses these estimates for decoding the PU's data and regenerating the time-domain interference. The duration of channel estimates reuse depends on the coherence time of the channel. Once the performance of the system degrades below a threshold value, the channel is re-estimated by blanking the transmission.

V. Results and Discussion

A. Simulation Parameters

The PU simulation parameters are based on ATSC 3.0 specification as mentioned in I while SU parameters are based on NR specification given in II.

TABLE I
PRIMARY (ATSC 3.0) PARAMETERS

Center Frequency	700 MHz
Sub-carrier spacing	843 Hz
Sampling Rate	6.912 MHz
CP length	192
FFT size	8192
Active Subcarriers	6913
Pilot pattern	SP16_2

TABLE II
SECONDARY (NEW RADIO LIKE) PARAMETERS

Center Frequency	700 MHz
Sub-carrier spacing	15 kHz
Sampling Rate	7.68 MHz
CP length	Normal
FFT size	512
Active Subcarriers	300
Pilot pattern	Front loaded

B. Effect of pilot contamination

The performance of SIC with and without pilot contamination is compared in figure 4. As can be observed that, for $\frac{P_{secondary}}{P_{ATSC}} < -25dB$, the SIC does not perform well due to pilot contamination which results into non zero mean square error (MSE) between the estimated and the actual channel

TABLE III
SECONDARY (NEW RADIO LIKE) SLOT SIZE CONFIGURATIONS

Configuration	Number of symbols in a slot
Cfg1	14
Cfg2	7
Cfg3	4
Cfg4	2

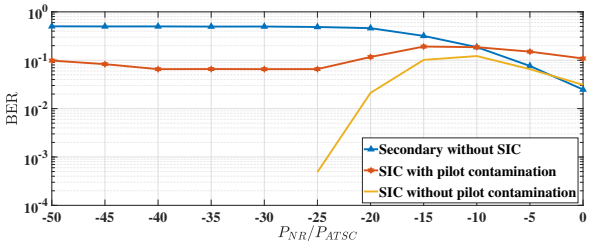

Fig. 4. Performance of SIC with and without pilot contamination for NR Configuration 1.

coeffecients. Additionally, it can also be observed that for $\frac{C}{I} = \frac{P_{secondary}}{P_{ATSC}} > -5dB$, the receiver with SIC performs poorer than receiver without SIC. This happens because at large $\frac{C}{I}$ values, ATSC 3.0 symbol error increases and thus, the reconstructed signal does not match the original interference values, as a result, subtracting it from the received signal further increases the interference power.

C. Performance of proposed schemes

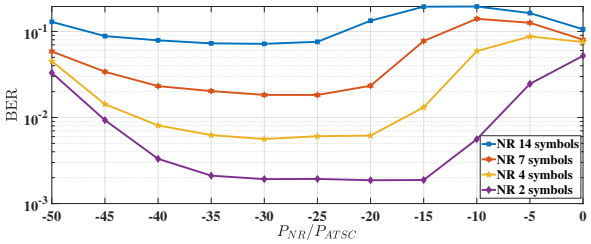

Fig. 5. Performance of SIC with reduced slot size.

The performance of the slot size-reduction scheme can be observed in figure 5. The slot sizes used for simulation are given in Table III. As can be seen from the figure, the slot size of 2 yields the best performance in terms of low BER among them. Even though the performance of the SU improves but the BER of the system is still $> 10^{-3}$. Additional improvement in performance can be obtained with the help of blanking scheme.

The performance of the proposed blanking scheme at the first symbol after blanking with doppler spreading of 2 Hz is shown in figure 6. From the graph it can be inferred that, the combination of slot size reduction and blanking technique provides tremendous improvement to the system performance at low values of $\frac{C}{I}$, particularly between -40 to -20 dB. Moreover, as $\frac{C}{I}$ further reduces below -40 dB, the BER starts

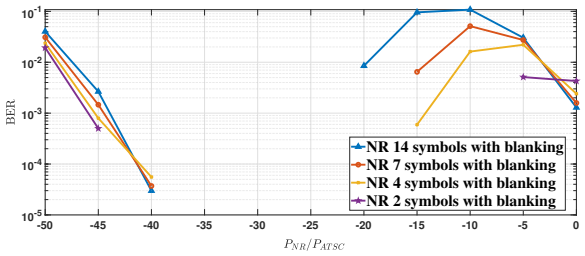

Fig. 6. Performance of SIC with blanking.

increasing, this happens because of ATSC's imperfect channel interpolation and decreasing channel correlation coupled with low values of $\frac{C}{I}$ results into a large value of residual interference in comparison to the SU signal power.

D. Channel estimation periodicity and Throughput analysis

The blanking approach works well so long as the channel has a high temporal correlation. The secondary system then needs to re-estimate the channel. Therefore, the estimation process can be viewed as a periodic process whose periodicity depends on the coherence time of the channel. The estimation periodicity $\mathbb{P}$ impacts the throughput of the system, if the periodicity is less, then the system will require frequent channel estimation attempts, which will degrade the system's throughput performance.

Figure 7 shows the channel estimation periodicity with 2 Hz

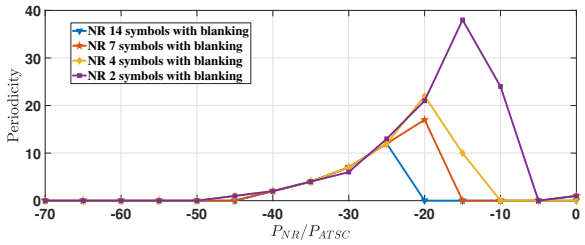

Fig. 7. Channel estimation period under 2 Hz Doppler spreading.

doppler spreading. For simulation, the threshold for channel re-estimation of SU receiver is kept at BER of 10^{-3}. From the figure, it can be observed that the maximum value of $\mathbb{P}$ decreases as the slot size increases.

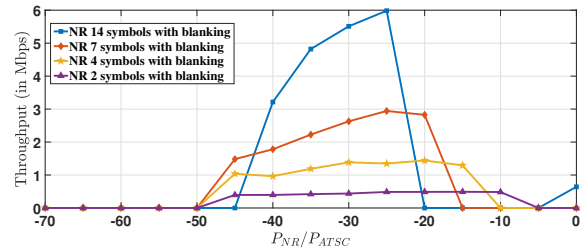

Fig. 8. Average throughput for 2 Hz Doppler spreading.

The throughput performance of the secondary system is shown in figure 8. It can be observed that the small slot size

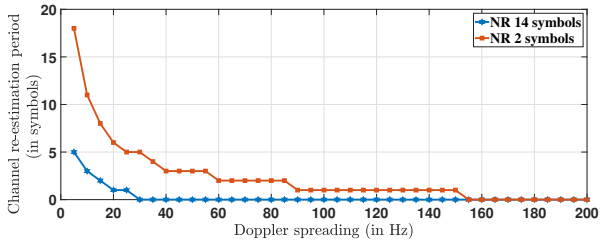

Fig. 9. Maximum value of channel estimation period versus Doppler spreading.

provides low but stable throughput over a wide range of $\frac{C}{I}$ values. It can also be noticed that even at low $\frac{C}{I}$ ratio of -40 dB, SU is able to support throughput which decreases with the decreasing length of slot size. The throughput of the SU system depends on symbol blanking frequency which in turns depend upon the doppler spreading in the system. The simulation results for estimation period $\mathbb{P}$ as a function of doppler spreading is shown in figure 9. It can be observed that as the doppler spreading increases, the channel re-estimation period decreases due to reduced channel coherence time.

VI. Conclusion

The paper has investigated the feasibility of secondary network communication over a coexisting ATSC 3.0 channel using Successive Interference Cancellation without affecting the ATSC 3.0 broadcast reception quality. It has been observed that the SIC fails to perform satisfactorily due to pilot contamination. Based on the observation, two schemes, namely, slot size reduction and symbol blanking, have been proposed and analyzed. The simulation results have shown that both the schemes provide significant improvement of the secondary receiver performance.

References

[1] S. Agarwal and S. De, "Rural Broadband Access via Clustered Collaborative Communication," in *IEEE/ACM Transactions on Networking*, vol. 26, no. 5, pp. 2160-2173, Oct. 2018.

[2] H. Bezabih, B. Ellingsaeter, J. Noll and T. T. Maseng, "Digital Broadcasting: Increasing the Available White Space Spectrum Using TV Receiver Information," in *IEEE Vehicular Technology Magazine*, vol. 7, no. 1, pp. 24-30, March 2012.

[3] Z. Zhao, M. C. Vuran, D. Batur and E. Ekici, "Shades of White: Impacts of Population Dynamics and TV Viewership on Available TV Spectrum," in *IEEE Transactions on Vehicular Technology*, vol. 68, no. 3, pp. 2427-2442, March 2019.

[4] P. Palka and P. Neumann, "Analyzing the availability of TV white spaces in dynamic broadcast," in *IEEE Transactions on Consumer Electronics*, vol. 60, no. 3, pp. 302-310, Aug. 2014.

[5] S. Agarwal and S. De, "eDSA: Energy-Efficient Dynamic Spectrum Access Protocols for Cognitive Radio Networks," in *IEEE Transactions on Mobile Computing*, vol. 15, no. 12, pp. 3057-3071, Dec. 2016.

[6] S. Agarwal and S. De, "Cognitive Multihoming System for Energy and Cost Aware Video Transmission," in *IEEE Transactions on Cognitive Communications and Networking*, vol. 2, no. 3, pp. 316-329, Sept. 2016.

[7] S. Agarwal and S. De, "Impact of Channel Switching in Energy Constrained Cognitive Radio Networks," in *IEEE Communications Letters*, vol. 19, no. 6, pp. 977-980, June 2015.

[8] S. Debroy, S. De and M. Chatterjee, "Contention based multi-channel MAC protocol for distributed cognitive radio networks," *Proc. IEEE Global Commun. Conf. (GLOBECOM)*, 2013, pp. 1221-1226.

[9] G. Martínez-Pinzón, N. Cardona, C. Garcia-Pardo, A. Fornés-Leal, and J. A. Ribadeneira-Ramírez, "Spectrum Sharing for LTE-A and DTT: Field Trials of an Indoor LTE-A Femtocell in DVB-T2 Service Area," *IEEE Trans. Broadcast.*, vol. 62, no. 3, pp. 552-561, Sept. 2016.

[10] V. Popescu, M. Fadda, M. Murroni, J. Morgade and P. Angueira, "Co-Channel and Adjacent Channel Interference and Protection Issues for DVB-T2 and IEEE 802.22 WRAN Operation," in *IEEE Transactions on Broadcasting*, vol. 60, no. 4, pp. 693-700, Dec. 2014.

[11] L. Polak, O. Kaller, L. Klozar, and J. Prokopec, "Exploring and measuring the co-existence between LTE and DVB-T2-Lite services," in *Proc. Intl. Conf. Telecommun. Sig. Process. (TSP)*, 2013, pp. 316-320.

[12] A. Thakur, S. De, and G. -M. Muntean, "Co-Channel Secondary Deployment Over DTV Bands Using Reconfigurable Radios," *IEEE Trans. Veh. Technol.*, vol. 69, no. 10, pp. 12202-12215, Oct. 2020.

[13] A. Thakur and S. De, "On Deploying Secondary Networks in Co-channel Bands with DTV Networks," in *IEEE Transactions on Vehicular Technology*.

[14] J. Lee, J. G. Andrews, and D. Hong, "The Effect of Interference Cancellation on Spectrum-Sharing Transmission Capacity," in *Proc. IEEE Intl. Conf. Commun. (ICC)*, 2011, pp. 1-5.

[15] S. Gollakota, F. Adib, D. Katabi, and S. Seshan, "Clearing the RF smog: Making 802.11n robust to cross-technology interference," *SIGCOMM Comput. Commun. Rev.*, vol. 41, no. 4, pp. 170–181, Aug. 2011.

[16] Y. Yubo, Y. Panlong, L. Xiangyang, T. Yue, Z. Lan, and Y. Lizhao, "ZIMO: building cross-technology MIMO to harmonize Zigbee smog with WiFi flash without intervention," in *Proc. ACM MobiCom*, 2013.

[17] S. Yun and L. Qiu, "Supporting WiFi and LTE co-existence," in *Proc. IEEE INFOCOM*, 2015, pp. 810-818.

[18] X. Zhang, L. Zhang, P. Xiao, D. Ma, J. Wei, and Y. Xin, "Mixed Numerologies Interference Analysis and Inter-Numerology Interference Cancellation for Windowed OFDM Systems," *IEEE Trans. Veh. Technol.*, vol. 67, no. 8, pp. 7047-7061, Aug. 2018.

[19] S. McWade, M. F. Flanagan, L. Zhang, and A. Farhang, "Interference and Rate Analysis of Multinumerology NOMA," in *Proc. IEEE Intl. Conf. Commun. (ICC)*, 2020, pp. 1-6.

[20] Y. Beyene, K. Ruttik and R. Jäntti, "Effect of secondary transmission on primary pilot carriers in overlay cognitive radios," in *Proc. Intl. Conf. on Cognitive Radio Oriented Wireless Networks (CROWNCOM)*, 2013, pp. 111-116.

[21] L. Fay, L. Michael, D. Gómez-Barquero, N. Ammar and M. W. Caldwell, "An Overview of the ATSC 3.0 Physical Layer Specification," in *IEEE Transactions on Broadcasting*, vol. 62, no. 1, pp. 159-171, 2016.

[22] M. Simon, E. Kofi, L. Libin and M. Aitken, "ATSC 3.0 Broadcast 5G Unicast Heterogeneous Network Converged Services Starting Release 16," in *IEEE Transactions on Broadcasting* vol. 66, no. 2, pp. 449-458, 2020.